Chem. Chem. Technol., 2023,
Vol. 17, No. 1, pp. 118–125

Chemistry

IMPROVEMENT OF ELECTRICAL CONDUCTIVITY AND THERMAL STABILITY OF POLYANILINE-MAGHNITE NANOCOMPOSITES

Nora Ouis[1,2,✉], Assia Belarbi[2], Salima Mesli[3], Nassira Benharrats[2]

https://doi.org/10.23939/chcht17.01.118

Abstract. A new nanocomposite based on conducting polyaniline (PANI) and Algerian montmorillonite clay dubbed Maghnite is proposed to combine conducting and thermal properties (Mag). The PANI-Mag nanocomposites samples were made by *in situ* polymerization with CTABr (cetyl trimethyl ammonium bromide) as the clay galleries' organomodifier. In terms of the PANI-Mag ratio, the electrical and thermal properties of the obtained nanocomposites are investigated. As the amount of Maghnite in the nanocomposite increases, thermal stability improves noticeably, as measured by thermal gravimetric analysis. The electric conductivity of nanocomposites is lower than that of free PANI. As the device is loaded with 5 % clay, the conductivity begins to percolate and decreases by many orders of magnitude. The findings show that the conductivity of nanocomposites is largely independent of clay loading and dispersion.

Keywords: intercalated, exfoliated structure, clay, conductor polymer, thermal properties.

1. Introduction

It is well known that clay particles are dispersed in a polymeric matrix to create several nanocomposites based on polymers. The integration of nanocharges into polymeric materials is well known to cause significant changes in their mechanical,[1] thermal,[2] electronic,[3] and barrier[4] properties.

For conducting matrix nanocomposites, preparation can be accomplished by comparing two parameters: the electrical conductivity, which can be monitored during the polymerization process, and the dispersion of clay nanoparticles inside the polymer, which can be controlled by vigorous stirring to increase the interactions between the two phases. The sizes and shapes of nanoparticles must also be considered.

Based on these observations, we have anticipated the synthesis of nanocomposites based on polyaniline and Maghnite, starting by the organophilization of Maghnite galleries to improve the affinity between the hydrophobic monomer and the hydrophilic clay particles.

The sodium cations of the monoionic Na-Maghnite will be exchanged with alkylammonium chains. In the presence of organoclay particles, the conductive polyaniline Emeraldine Salt (PANI-ES) will be prepared. According to the experimental protocol stated by MacDiarmid,[5] polyaniline will be synthesized by chemical oxidation of aniline monomer with sodium persulfate in acidic aqueous solution.

2. Experimental

2.1. Materials

ENOF Algeria generated the initial Maghnite (Mag).[6,7] Table 1 contains information on chemical composition, specific surface area, and CEC. Aldrich's cetyl trimethyl ammonium bromide (CTABr) and sodium persulfate ($Na_2S_2O_8$) were used as received. Before use, aniline (Biochem-Chemopharma) was distilled under vacuum and purified. Almost all of the experiments were done with deionized water.

2.2. Methods

The FT-IR spectra were recorded in the range of 4000–400 cm^{-1}using a Perkin-Elmer 1730 infrared Fourier transform spectrometer through the KBr pellet technique. The XRD spectra were obtained using a Philips PW 1710 diffractometer with Cu K radiation at 40 kV and 30 mA, a 2-angle range of 2° to 40°, and a scanning rate of 2°/min. Thermal gravimetric analyses were performed on Setaram Labsys apparatus with the heating rate of 10 K/min. The DSC 200 PC NETZSCH apparatus was used to record the Differential Scanning Calorimetric (DSC). Temperature was measured in the range of 293 K to 723 K, with the

[1] Unité de Chimie, Faculté de Médecine, Université 1 Oran, BP 1510 Al M'naouer Oran, 31000, Algérie
[2] L.P.P.M.C.A. Université des Sciences et de la Technologie, M. Boudiaf BP 1505 Al M'naouer Oran, 31000, Algérie
[3] Laboratoire de Chimie des matériaux, BP 1524 Oran, El Mnaouer, Algérie
✉ *nora_ouis@yahoo.fr*

heating rate of 283 K/min. Electric conductivity was measured using the four-probe technique for pellets of 13 mm diameter and compressed at 700 MPa. In 1M of sulfuric acid solution, cyclic voltametry was performed with a reversible Hydrogen electrode as the reference electrode and Pt foil as the counter electrode at a scanning rate of 50 mVs^{-1}. The microstructure of PANI-Mag nanocomposite is examined by TEM (JOEL JEM 2011).

Table 1. Characterization of Mag: chemical composition, specific surface area and CEC

	SiO_2	Al_2O_3	Fe_2O_3	MgO	CaO	Na_2O	K_2O	TiO_2	SO_3	As	PF*
Mag	69.3	14.67	1.16	1.07	0.3	0.5	0.79	0.16	0.91	0.05	11
	Specific surface area= 760 m²/g					CEC = 110 meq/100g					

2.3. Clay Organophilization

To the suspension solution of Na-Mag (sodium Maghnite) (5 g) in deionized water (250 mL) a solution of CTABr (15 mmol) was added dropwise under stirring. The stirring was continued for 3 h at room temperature, then the mixture was heated at 353 K for 4 hr. The exchanged clay was filtered and washed with deionized water till the disappearance of bromide as indicated by $AgNO_3$ test. The lipophilic clay (Org Mag) was dried and crushed with extreme care so that the surface structure is maintained. The particles produced are extremely fine (less than 0.8 m), leading to better dispersion.

2.4. Synthesis of PANI-Org Mag nanocomposites

2.4.1. Synthesis of PANI

According to a molar $Na_2S_2O_8$/aniline ratio of 0.25, sodium persulfate ($Na_2S_2O_8$) was added to 250 mL HCl 1M aqueous solution and 68 mmol aniline monomer. Then, the reaction temperature was kept at 278 K for 8 hr. The conductive form of polyaniline is present in the obtained dark green powder. The resulted stock is rinsed twice with a 1M HCl concentrated solution and dried for three days under vacuum at 343 K.

2.4.2. Synthesis of nanocomposite

In a 1M HCl aqueous solution, a desired amount of functionalized clay (Org Mag) was dispersed, the suspension solution was mechanically stirred for 1 hr at room temperature, to ensure that the clay particles were well dispersed. The colloidal suspension received 68 mmol of aniline monomer. Then, the mixture was cooled to 278 K and stirred for 24 hr in order to intercalate the monomer in the clay galleries. The dispersion was then gradually supplemented with 17 mmol sodium persulfate. To make PANI–clay nanocomposites, the polymerization reaction was carried out for 8 hr. To extract the adsorbed salts, the nanocomposites were filtered and suspended in distilled water with mechanical stirring for 1 hour, then washed with methanol and dried in dehydrative oven.

3. Results and Discussion

3.1. Functionalization of Mag by CTABr

FT-IR analysis. The Maghnite clay organomodifications were evidenced by the IR spectral data as shown in Fig. 1, which compare the IR spectrum of raw with its analogues organomodified Maghnite. Thus, the IR of raw exhibited a characteristic band of montmorillonite, the hydroxyl absorption band was observed at 3620 cm^{-1}, while the band recoded around 3370 cm^{-1} was attributed to the molecular adsorbed H_2O stretching. In addition, the band belonging to Si–O bonds was observed at 1030 cm^{-1}. While the IR spectrum of the resulted organomodified Maghnite revealed new absorption bands confirming the success of the maghnite clay organomodification. The absorption bands appeared at 2925, 2852 and 1480 cm^{-1} were attributed to CH_2 stretching and bending, respectively[8,9] confirming the presence of CTABr with the clay particles but no clear information can be concluded concerning the relative position of the organic-inorganic phases.

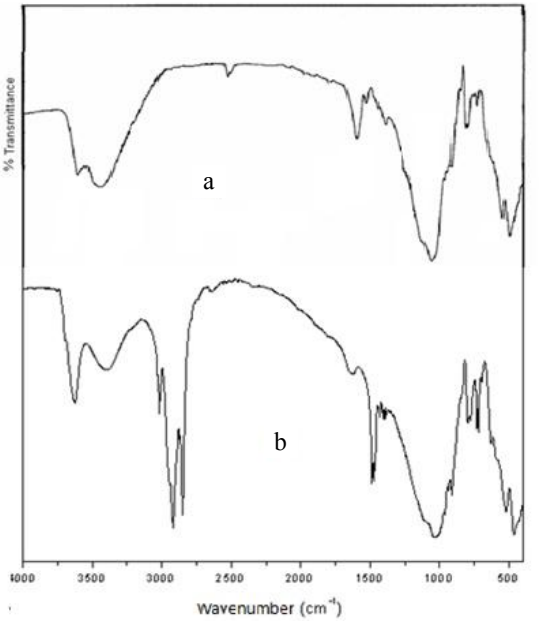

Fig. 1. FTIR spectra of (a) Na-Mag and (b) CTABr-Mag

X Ray Diffraction analysis. To confirm the relative locations of PANI and Maghnite, an XRD analysis was carried out and revealed that the two-dimensional layers of montmorillonite are formed by fusing two silica tetrahedral sheets to an edge-shared octahedral sheet of aluminium hydroxide.[10] The interaction of weak dipolar or Van Der Waals forces layers causes crystal cohesion. The raw Maghnite has a hydrophilic surface. The cation exchange of sodium cations for alkylamonium cations increases the hydrophobicity of the clay base, allowing the clay particles to spread easily in the organic monomer. Fig. 2 showed the typical XRD patterns of CTABr–Mag. Thus, in the Org-Mag study, the d001 reflection appeared at 2θ = 4.0 16 with a spacing value of around 22. Na-Mag has a basal spacing value of 13. While alkylamonium cations are clearly intercalated into the interlayer space during the ion exchange process, replacing Na^+. The basal spacing change indicates that CTABr has been successfully intercalated into the interlayer spaces.

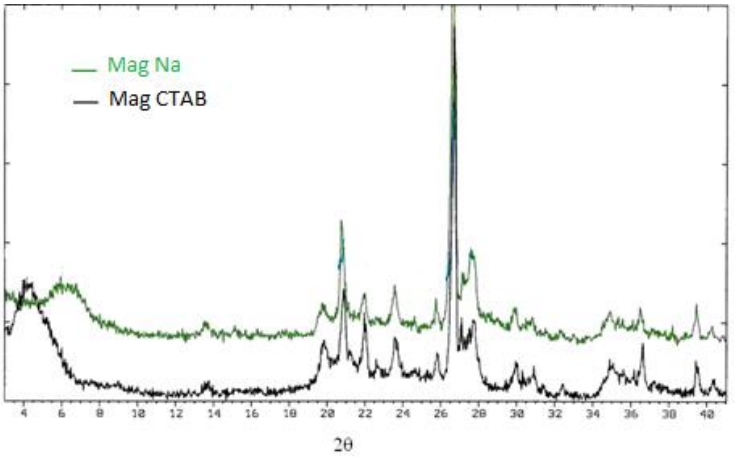

Fig. 2. XRD patterns of (a) Na-Mag and (b) CTABr-Mag

3.2. Nanocomposites characterizations

FTIR Analysis. The FTIR spectra of the PANI and PANI-Mag nanocomposite samples are illustrated in Fig. 3a and 3b, respectively ranging from 600 to 1800 cm^{-1}. Thus, the FTIR spectrum of PANI showed clearly the presence of a diagnostic absorption band between 3500–3300 cm^{-1} belonging to the N–H bond stretching of benzenoid or quinoid rings.[11-13] In addition, characteristic bands were observed at 1610, 1480 and 1310 cm^{-1} and were attributed to the C=C stretching of benzene ring and C-N group, respectively (Fig. 3a).[14] The bending of the aromatic hydrogens (Ar-H) in plane and out of plane of 1,4-disubstitution benzene were recorded around 1150 and 820 cm^{-1}, respectively.[15] While the absorption band observed at 1242 cm^{-1} was in obvious of conducting PANI ES form.[16]

On the other hand, the IR spectrum of the 5 % loaded nanocomposite was depicted in Fig. 3b. Its investigation showed clearly the shift of the absorption bands toward lower values compared to its respected PANI (1580, 1500 and 1300 cm^{-1}). The spectrum also exhibited a weak band at 1150 cm^{-1}assigned to the bending of the aromatic C–H. The presence of Maghnite in this area is associated to the shoulder at 1050 cm^{-1}, which corresponds to Si-O bonds.

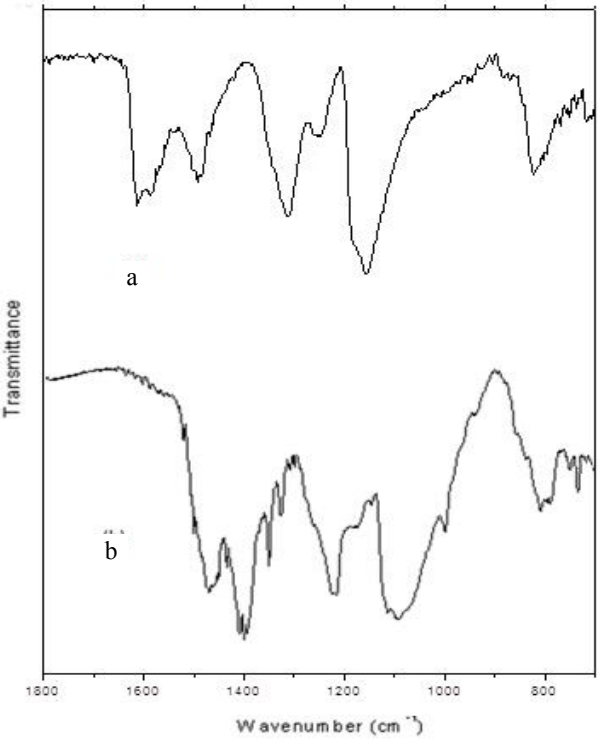

Fig. 3. FTIR Spectra of (a) PANI and (b) PANI-Mag loaded at 5 %

X-Ray Diffraction. Since a more highly ordered system may show a metal-like conducting state,[17] crystallinity and orientation of conducting polymers have been investigated. It is well known that the polyaniline is a semi crystalline polymer with amorphous and crystalline zones. In XRD analysis, such structure shows a strong and relatively sharp peak for the four peaks centered at 2θ = 9, 15, 21, and 25° were observed in the X-ray pattern of PANI samples (Fig. 4a). The characteristic distance between the ring planes of benzene in adjacent chains, or the near contact inter-chain distance,[18] is described by the peak at 2θ = 21°.

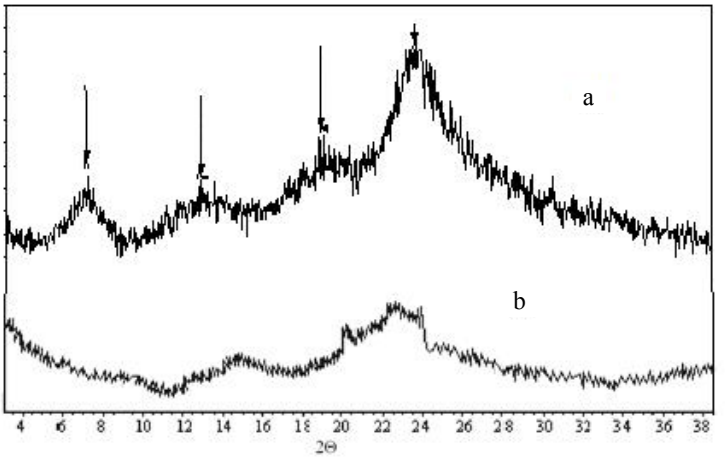

Fig. 4. XRD patterns of (a) PANI and (b) PANI-Mag loaded at 5 %

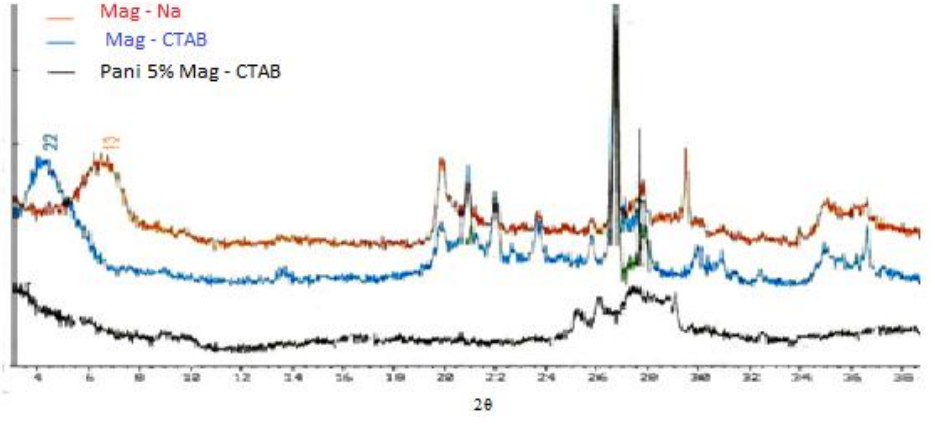

Fig. 5. XRD patterns of MMT-Na, MMT-CTAB and PANI-Mag loaded at 5 %

The peak of 2θ = 25° is higher than that of 2θ = 21°, suggesting that PANI ES is heavily doped.[19] The PANI-Mag 5 wt % loaded nanocomposite diffractogram (Fig. 4b) shows one peak at 2θ ≃ 25°, with high PANI diffraction peaks dominant and no characteristic Maghnite diffraction peak noticeable. This means that the clay layers have lost their structure registry and have been exfoliated into nanolayers in the polymer matrix, resulting in silicate dispersion at the molecular level. The strong interaction between aniline and organomodified Maghnite, which is due to the migration of monomer into the clay galleries due to the presence of sufficiently hydrophobicity to accommodate it, may be responsible for Maghnite exfoliation in polyaniline matrix (Fig. 5).

Thermal Analysis. To control the effect on the thermal properties of the clay nanolayers dispersed in the polyaniline matrix, DSC and Thermogravimetric analysis (TGA) were documented for PANI and PAN-Mag nanocomposites.

(a) DSC: In the DSC analysis curves Figs. 6a and 6b, the thermal behavior of PANI and PANI–Mag nanocomposite at 5 % clay loading is shown. Fig. 6a shows a thermogram that is typical of PANI.[20,21] At around 373 K, the first endothermic peak corresponds to physisorbed water. The second, at 518 K, corresponds to polymeric chain relaxation,[20,22] followed by a wide exothermic one at 568 K, which corresponds to chain cross-linking just before polymer decomposition, which occurs at 663 K.[23]

The DSC thermogram of the 5 % PANI-Mag loading nanocomposite is shown in Fig. 6b. The shoulder at 503 K could be linked to the chains initial relaxation at 518 K in pure PANI. This change is caused by the presence of clay particles, which prevent polymeric chains for freely moving. The CTAB 683 K is related to the endothermic peak at 538 K. At 713 K, the onset of temperature decomposition is also delayed.[24]

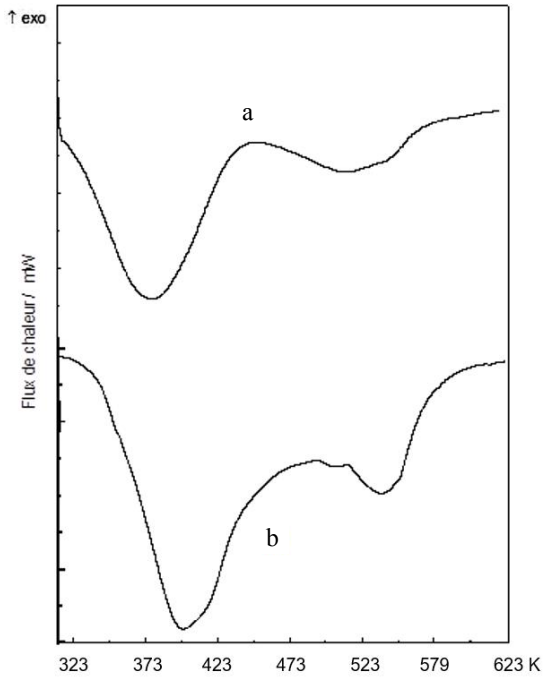

Fig. 6. DSC thermogram of (a) PANI and (b) PANI-Mag loading at 5 %

(b) Thermogrativemetric Analysis: The thermal stabilities of PANI and PANI – Mag nanocomposites are shown in Fig. 7 as a function of Maghnite material. For all of the samples examined, a three-step weight loss procedure can be seen.

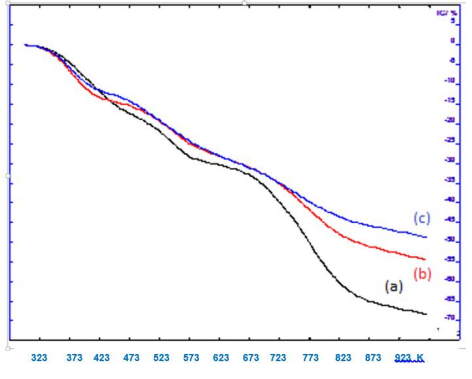

Fig. 7. TG curves of (a) PANI, (b) and (c) PANI- Magloaded at 5 % and 10 % respectively

Three weight loss peaks can be seen on the PANI curve (Fig. 7a). The first stage shows an 18 % weight loss from 353 K to 393 K, which is caused by physisorbed water desorption. Between 497 K and 604 K, the second one occurs at a rate of about 11 %. It is due to the removal of H^+, which is paired with Cl^- anions, resulting in the elimination of HCl.[25-27] The third and most significant weight loss is around 38 percent and is attributed to polymeric chain degradation.[28]

The nanocomposites curves showed in Figs. 7b and 7c showed three distinct steps, the first of which corresponds to the removal of physisorbed water molecules. The second is more noticeable than in PANI. For 5 % and 10 % clay loading samples, weight loss of 14 and 16 % were observed at 473 K up to 603 K, respectively.

This has to do with the decomposition of organic surfactants used for Maghnite surface treatment and the removal of protons from PANI chains. With increasing clay content, the temperatures of the third weight loss increased, reaching 700 and 713 K, corresponding to 20 and 26 percent weight loss, respectively. The thermal stability of the nanocomposites has increased, as can be shown. Lee and Char[29] published similar findings of higher thermal decomposition temperatures of intercalated PANI–clay nanocomposites. Due to the homogeneous distribution of the silicate sheets into the matrix, the nanocomposites exhibit a delayed decomposition compared to PANI, which improved the thermal properties of the nanocomposites.

Electrical properties

Cyclic voltammetry: To study the electrochemical behavior of PANI and PANI-Mag nanocomposite, a conventional cell of three electrodes was used. Polymer films were obtained by casting a drop of in NMP over a platinum disk electrode and heating with an infrared lamp to remove the solvent. Fig. 8 shows similar electrochemical response for the two samples in 1M H_2SO_4 solution. The current densities have been normalized in order to compare two polymers electrochemical behaviours. PANI and PANI- Mag nanocomposite exhibit two anodic peaks around 0.46 and 0.96 V. On the reverse scan, two reduction peaks around 0.3 V and 0.92 V are observed. These results concur with those published in the literature.[30-32]

Electrical Conductivity: In order to assess the percolating threshold for PANI-Mag nanocomposites, electric measurements were taken. For all possible applications, it is critical to combine thermal stability with good electric conductivity. Fig. 9 shows the conductivity data obtained for PANI-Mag nanocomposites. The conductivity of the PANI–Mag nanocomposite has decreased, as shown. The percolation threshold appears to be some-

where near 5 %. Maghnite nanocomposites have a lower conductivity than free PANI. As the amount of insulate clay in nanocomposites is increased, the electrical conductivity of the composites decreases. When the polymer/clay mass ratio is increased, conductivity values of PANI-Mag nanocomposites range from 1 to 10^{-3} S·cm^{-1}. The conductivity drops several orders of magnitude when a critical ratio, or percolation threshold, is reached (5 percent in this study). In the nanocomposite, the PANI conductive network breaks down, and the conductivity plummets.

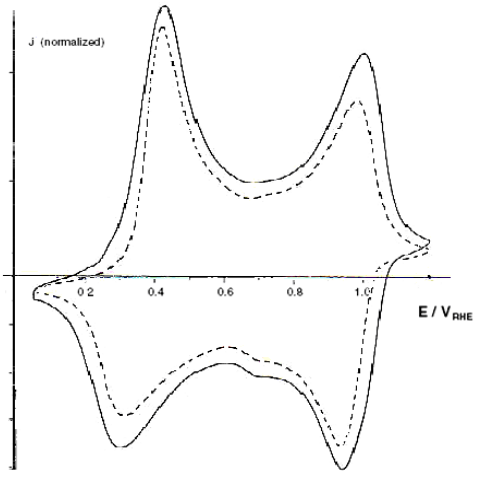

Fig. 8. Cyclic voltamograms for Pt electrodes covered by PANI-Mag nanocomposite (5 %) (solid line) and PANI ES (dashed line) in H_2SO_4 solution

The main cause of the conductivity decrease in this case is clay particles. Interchain transport is limited due to the lack of communication between PANI chains. Effect of temperature on electrical conductivity: Two sets of experiments were carried out in order to investigate the effect of temperature on the electrical conductivity of nanocomposite as compared to raw PANI. The first involves aging synthesized samples at 298 K for 15, 30, 45, and 90 days, and the second involves aging the samples at 423 K in an oven for 15, 30, 45, and 90 days. Taking into consideration, the second temperature was chosen.

The results are shown in Figs. 10a and b. As can be seen, at room temperature, the electrical conductivity of the selected samples (PANI, nanocomposite 3 and 5 percent loaded) exhibits the same behavior, *i.e.*, it decreases slowly over time. The decrease in loaded samples is less important than the decrease in pure samples.

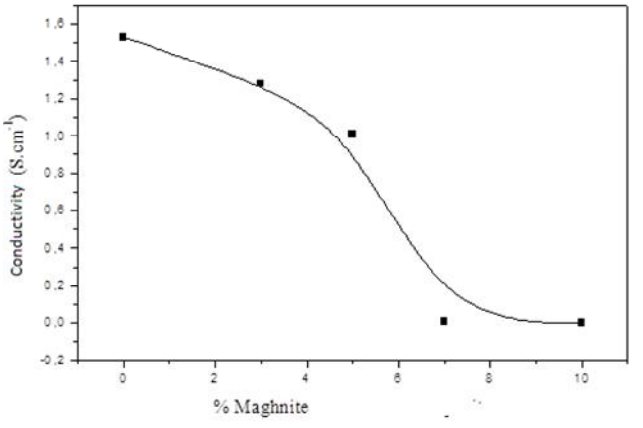

Fig. 9. Electrical conductivity against Maghnite content in nanocomposites

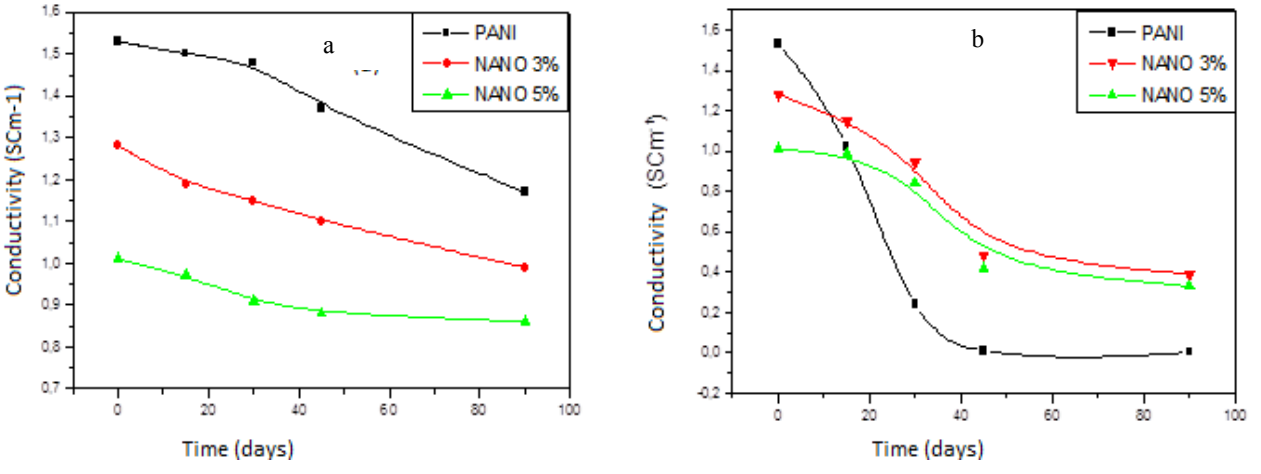

Fig. 10. Electrical conductivity of PANI and PANI-Mag nanocomposites (3 %, 5 %) according to time (a) at T = 298 K and (b) at T = 423 K

Curve profiles diverge at higher temperatures (423 K) showed that at an early point, the pure PANI conductivity shuts down. After 30 days of temperature exposure, it dramatically decreases; the loss is more than 80 %. This parameter, on the other hand, remains constant in nanocomposites and decreases slowly. For the 5 % loaded samples, the conductivity loss reached 67 % after 90 days. We may logically conclude that the conducting nanocomposites exhibited a higher stability than PANI. These good electrical properties of nanocomposites are due to their exfoliated structure confirmed by X-ray diffraction (Figs. 4 and 5) and transmission electron microscope (Fig. 11).

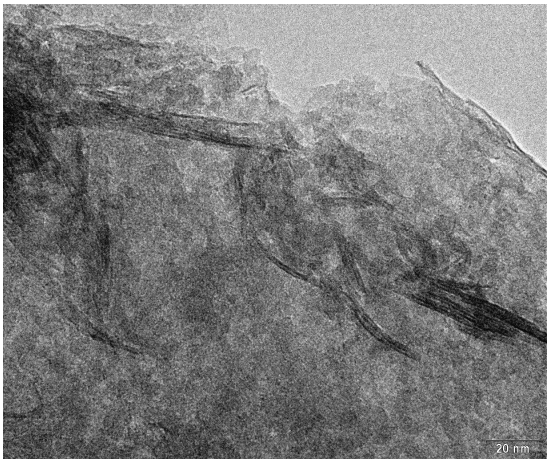

Fig. 11. TEM image of nanoPANI-Mag 5 %

4. Conclusions

In the work we successfully prepared hybrid organic–inorganic nanocomposites from PANI-Maghnite with good thermal stability and good electric conductivity. The clay layers are exfoliated in the polymeric matrix as evidenced by the XRD results of the collected nanocomposites. Based on the TGA, DSC, and conductivity data, as well as the thermal and electrical behavior, we conclude that the PANI-Mag nanocomposites change with clay content. Clay particles in nanocomposites improve the PANI's thermal stability, delaying its decomposition. Maghnite's stability increases as its concentration increases.

PANI showed a good electronic conduction. PANI-Mag composite conductivity values changed from 1 to 10^{-3} S·cm^{-1}. Nanocomposites with a loading of less than 5 % have conductivity similar to PANI. Above this point, the presence of clay particles disrupts the delocalization of electron transport in the polymeric chains, resulting in a loss of conductivity. The effect of temperature on conductivity was also investigated, and it was revealed that nanocomposite containing up to 5 % Maghnite can withstand high temperatures.

References

[1] Gonzalez, L.; Lafleur, P.; Lozano, T.; Morales, A.B.; Garcia, R.; Angeles, M.; Rodriguez, F.; Sanchez, S. Mechanical and Thermal Properties of Polypropylene/Montmorillonite Nanocomposites Using Stearic Acid as Both an Interface and a Clay Surface Modifier. *Polym. Compos.* **2014**, *35*, 1-9. https://doi.org/10.1002/pc.22627

[2] Valandro, S.R.; Lombardo, P.C.; Poli, A.L.; Horn Jr., M.A.; Neumann, M.G.; Cavalheiro, C.C.S. Thermal Properties of Poly (Methyl Methacrylate)/Organomodified Montmorillonite Nanocomposites Obtained by *in situ* Photopolymerization. *Mater. Res.* **2014**, *17*, 265-270. https://doi.org/10.1590/S1516-14392013005000173

[3] Dhatarwal, P.; Sengwa, R.J.; Choudhary S. Effect of Intercalated and Exfoliated Montmorillonite Clay on the Structural, Dielectric and Electrical Properties of Plasticized Nanocomposite Solid Polymer Electrolytes. *Compos. Commun.* **2017**, *5*, 1-7. https://doi.org/10.1016/j.coco.2017.05.001

[4] Cui, Y.; Kumar, S.; Kona, B.R.; van Houcke, D. Gas Barrier Properties of Polymer/Clay Nanocomposites. *RSC Adv.* **2015**, *5*, 63669-63690. https://dx.doi.org/10.1039/c5ra10333a

[5] MacDiarmid, A.G. Nobel Lecture: "Synthetic Metals": A Novel Role for Organic Polymers. *Rev. Mod. Phys.* **2001**, *73*, 701-712. https://doi.org/10.1103/RevModPhys.73.701

[6] Belbachir, M.; Bensaoula, A. Composition and Method for Catalysis Using Bentonite. US 7, 094, 823 B2, January 1, 2006.

[7] Haoue, S.; Derdar, H.; Belbachir, M.; Harrane, A. A New Green Catalyst for Synthesis of bis-Macromonomers of Polyethylene Glycol (PEG). *Chem. Chem. Technol.* **2020**, *14*, 468-473. https://doi.org/10.23939/chcht14.04.468

[8] Zhu, J.; He, H.; Zhu, L.; Wen, X.; Deng, F. Characterization of Organic Phases in the Interlayer of Montmorillonite Using FTIR and 13C NMR. *J. Colloid Interface Sci.* **2005**, *286*, 239-244. https://doi.org/10.1016/j.jcis.2004.12.048

[9] Zhu, L.; Zhu, R.; Xu, L.; Ruan, X. Influence of Clay Charge Densities and Surfactant Loading Amount on the Microstructure of CTMA–Montmorillonite Hybrids. *Colloids Surf. A: Physicochem. Eng. Asp.* **2007**, *304*, 41-48. https://doi.org/10.1016/j.colsurfa.2007.04.019

[10] Caillere, S.; Henin, S.; Rautureau, M. *Minéralogie des argiles*; Masson: Paris, 1982.

[11] Tang, J.; Jing, X.; Wang, B.; Wang, F. Infrared Spectra of Soluble Polyaniline. *Synth. Met.* **1988**, *24*, 231-238. https://doi.org/10.1016/0379-6779(88)90261-5

[12] Ghosh, M.; Meikap, A.K.; Chattopadhyay, S.K.; Chatterjee, S. Low Temperature Transport Properties of Cl-Doped Conducting Polyaniline. *J. Phys. Chem. Solids* **2001**, *62*, 475-484. https://doi.org/10.1016/S0022-3697(00)00189-X

[13] Yan, H.; Toshima, N. Chemical Preparation of Polyaniline and its Derivatives by Using Cerium(IV) Sulfate. *Synth. Met.* **1995**, *69*, 151-152. https://doi.org/10.1016/0379-6779(94)02398-I

[14] Rout, T.K.; Jha, G.; Singh, A.K.; Bandyopadhyay, N.; Mohanty, O.N. Development of Conducting Polyaniline Coating: A Novel Approach to Superior Corrosion Resistance. *Surf. Coat. Technol.* **2003**, *167*, 16-24. https://doi.org/10.1016/S0257-8972(02)00862-9

[15] Ruckenstein, E.; Yang, S. An Emulsion Pathway to Electrically Conductive Polyaniline-Polystyrene Composites. *Synth. Met*. **1993**, *53*, 283-292. https://doi.org/10.1016/0379-6779(93)91097-L
[16] Khiew, P.S.; Huang, N.M.; Radiman, S.; Ahmad, Md.S. Synthesis and Characterization of Conducting Polyaniline-Coated Cadmium Sulphide Nanocomposites in Reverse Microemulsion. *Mater. Lett*. **2004**, *58*, 516-521. https://doi.org/10.1016/S0167-577X(03)00537-8
[17] Li, Q.; Cruz, L.; Philips, P. Granular-Rod Model for Electronic Conduction in Polyaniline. *Phys. Rev. B* **1993**, *47*, 1840-1845. https://doi.org/10.1103/PhysRevB.47.1840
[18] Pouget, J.P.; Hsu, C.-H.; MacDiarmid, A.G.; Epstein, A.J. Structural Investigation of Metallic PAN-CSA and Some of its Derivatives. *Synth. Met*. **1995**, *69*, 119-120. https://doi.org/10.1016/0379-6779(94)02382-9
[19] Pouget, J.P.; Jozefowicz, M.E.; Epstein, A.J.; Tang, X.; MacDiarmid, A.G. X-Ray Structure of Polyaniline. *Macromolecules* **1991**, *24*, 779-789. https://doi.org/10.1021/ma00003a022
[20] Chan, H.S.O.; Ng, S.C.; Sim, W.S.; Seow, S.H.; Tan, K.L.; Tan, B.T.G. Synthesis and Characterization of Conducting poly(o-Aminobenzyl Alcohol) and its Copolymers with Aniline. *Macromolecules* **1993**, *26*, 144-150. https://doi.org/10.1021/ma00053a022
[21] Tsocheva, D.; ZIatkov, T.; Terlemezyan, L. Thermoanalytical Studies of Polyaniline 'Emeraldine base'. *J. Therm. Anal. Calorim*. **1998**, *53*, 895-904. https://doi.org/10.1023/A:1010146619792
[22] Ghosh, P.; Chakrabarti, A.; Siddhanta, S.K. Studies on Stable Aqueous Polyaniline Prepared with the Use of Polyacrylamide as the Water Soluble Support Polymer. *Eur. Polym. J*. **1999**, *35*, 803-813. https://doi.org/10.1016/S0014-3057(98)00065-2
[23] Schemid, A.L.; Córdoba de Torresi, S.I.; Bassetto, A.N.; Carlos, I.A. Structural, Morphological and Spectroelectrochemical Characterization of poly (2-Ethyl Aniline). *J. Braz. Chem. Soc*. **2000**, *11*, 317-323. https://doi.org/10.1590/S0103-50532000000300020
[24] Yoshimoto, S.; Ohashi, F.; Ohnishi, Y.; Nonami, T. Synthesis of Polyaniline–Montmorillonite Nanocomposites by the Mechanochemical Intercalation Method. *Synth. Met*. **2004**, *145*, 265-270. https://doi.org/10.1016/j.synthmet.2004.05.011
[25] Chan, H.S.O.; Teo, M.Y.B.; Khor, E., Lim, C.N. Thermal Analysis of Conducting Polymers Part I. *Journal of Thermal Analysis* **1989**, *35*, 765-774. https://doi.org/10.1007/BF02057231
[26] Neoh, K.G.; Kang, E.T.; Tan, K.L. Thermal Degradation of Leucoemeraldine, Emeraldine Base and their Complexes. *Thermochim. Acta* **1990**, *171*, 279-291. https://doi.org/10.1016/0040-6031(90)87027-A
[27] Oh, S.Y.; Koh, H.C.; Choi, J.W.; Rhee, H.-W.; Kim, H.S. Preparation and Properties of Electrically Conductive Polyaniline-Polystyrene Composites by in-situ Polymerization and Blending. *Polym. J*. **1997**, *29*, 404-409. https://doi.org/10.1295/polymj.29.404
[28] Wei, Y.; Jang, G.-W.; Hsueh, K.F.; Scheer, E.M.; MacDiarmid, A.G.; Epstein, A.J. Thermal Transitions and Mechanical Properties of Films of Chemically Prepared Polyaniline. *Polymer* **1992**, *33*, 314-322. https://doi.org/10.1016/0032-3861(92)90988-9
[29] Lee, D.; Char, K. Thermal Degradation Behavior of Polyaniline in Polyaniline/Na+-Montmorillonite Nanocomposites. *Polym. Degrad. Stab*. **2002**, *75*, 555-560. https://doi.org/10.1016/S0141-3910(01)00259-2
[30] Huang, W.-S.; Humphrey, B.D.; MacDiamid, A.G. Polyaniline, a Novel Conducting Polymer. Morphology and Chemistry of its Oxidation and Reduction in Aqueous Electrolytes. *J. Chem. Soc., Faraday trans. I* **1986**, *82*, 2385-2400. https://doi.org/10.1039/F19868202385
[31] Desilvestro, J.; Scheifele, W.; Hass, O. In Situ Determination of Gravimetric and Volumetric Charge Densities of Battery Electrodes: Polyaniline in Aqueous and Nonaqueous Electrolytes. *J. Electrochem. Soc*. **1992**, *139*, 2727. https://doi.org/10.1149/1.2068971
[32] Kobayashi, T.; Yoneyama, H.; Tamura, H. Oxidative Degradation Pathway of Polyaniline Film Electrodes. *J. Electroanal. Chem. Interfacial Electrochem*. **1984**, *177*, 293-297. https://doi.org/10.1016/0022-0728(84)80230-2

Received: March 08, 2021 / Revised: April 26, 2021 / Accepted: May 08, 2021

ПОКРАЩЕННЯ ЕЛЕКТРОПРОВІДНОСТІ ТА ТЕРМОСТІЙКОСТІ НАНОКОМПОЗИТІВ ПОЛІАНІЛІН-MAGHNITE

Анотація. *Одержано новий нанокомпозит на основі електропровідного поліаніліну (PANI) й алжирської монтморилонітової глини під назвою Maghnite, який поєднує електропровідні та теплові властивості (Mag). Зразки нанокомпозитів PANI-Mag синтезовано за допомогою in situ полімеризації в присутності ЦТАБ (цетилтриметиламоній броміду) як органомодифікатора галерей глини. Досліджено електричні та теплові властивості отриманих нанокомпозитів залежно від співвідношення PANI-Mag. Зі збільшенням кількості Maghnite в нанокомпозиті його термічна стабільність помітно покращується, як показано термогравіметричним аналізом. Електропровідність нанокомпозитів нижча, ніж у вільного PANI. За додавання 5 % глини провідність починає падати і зменшується на багато порядків. Одержані результати показують, що провідність нанокомпозитів не залежить істотно від вмісту та дисперсності глини.*

Ключові слова: *інтеркальована, розшарована структура, глина, електропровідний полімер, теплові властивості.*